

Liquid Surface Wave Band Structure Instabilities

Tom Chou

DAMTP, University of Cambridge, Cambridge CB3 9EW, ENGLAND

(October 6, 2018)

We use Bloch wavefunctions in a new way to study a *fluid* interfacial problem and find both linear oscillatory and nonoscillatory instabilities of the surface deformation. Underlying periodic flows, such as those arising in Rayleigh-Bénard cells, Langmuir circulation, and solar convection rolls are treated as regions of varying surface shear which scatter and refract surface capillary-gravity waves. We find that Bloch wavefunction decompositions of the surface deformation $\eta(\vec{r})$ and velocity potential $\varphi(\vec{r}, z)$ results in a nonhermitian secular matrix with an associated band structure that gives rise to extremely rich surface instabilities (complex frequencies). These are predominantly enhanced at certain Brillouin zone edges, particularly near Bragg planes corresponding to the periodicity determined by converging or diverging surface flows. The instabilities persist *even* when the dynamical effects of the upper fluid are neglected, in contrast to the uniform shear Kelvin-Helmholtz instability. The periodic flows can also couple with uniform shear and *suppress* standard Kelvin-Helmholtz(K-H) instabilities.

47.20.Ft, 47.20.Ma, 68.10.-m

Introduction - Regular fluid flow patterns are ubiquitous [1]. Periodic flows are typically the result of thermal and/or dynamical instabilities and can exist in parameter regimes prior to chaotic or turbulent flows. An example on laboratory scales is the well-known Rayleigh-Bénard convective instability [2]. Heating of a fluid layer from below provides buoyancy which induces the instability. As the instability develops, regular convective patterns in the form of rectangles and hexagons appear [2,3].

Another physical example of nearly periodic flows with a free surface occurs in Langmuir circulation (LC) windrows where wind stresses, turbulent stresses, and coriolis forces conspire to form convection rolls in the upper ocean [4,5]. These flows can be spatially periodic as often observed when the sea surface is contaminated by oil slicks or algae. The LC process is believed to be an important mechanism in thermal and chemical mixing in the upper ocean. Mechanisms of LC generation may involve the interaction of turbulent surface currents with surface waves which in turn mediate the wind stresses [5]. Refraction of largely irrotational surface waves from the underlying rotational Langmuir circulation rolls are thought to contribute to wave breaking and enhanced local wind stresses [5]. On an even larger scale are the approximately periodic solar convection cells in the solar convective zone. In this system, magnetic fields will likely also affect the surface wave dynamics [6].

Clearly, surface wave propagation and interfacial stability is an important aspect of stratified fluids with wide applicability. Oscillatory instabilities of the two-layer Bénard problem have been studied by considering all coupled modes, including thermal and Marangoni [3]. In the limiting one layer Rayleigh-Bénard problem, Benguria and Depassier [7] even find interfacial oscillatory instabilities for parameters *prior* to the onset of the periodic roll states. This occurs in the fixed lower temperature

and fixed upper thermal flux ensemble. In this Letter, we assume a pre-existing periodic flow and explore its dynamical effects on interfacial instabilities. By considering surface wave motions as a perturbation to the underlying mean flows, we treat the surface waves as being reflected or refracted much like wave scattering in optical, acoustic, or electronic solid state physics, where band structures have been calculated using linear eigenvalue analysis in various systems [8]. A related problem of periodic surface wave scatterers such as thin ice floes has been treated with similar methods [9]. Here the underlying flow is periodic so we use Bloch functions to describe the surface displacements and dynamic fluid pressure and derive a generalized quadratic eigenvalue equation with a nonhermitian operator. In addition to nontrivial “band structure” we find a complex eigenvalue spectrum corresponding to linear instabilities with rich behavior. We show the existence of interfacial instabilities in the one layer problem, as well as modifications to the stability regions of uniform shear in the two-layer problem (K-H instability) when an additional periodic flow is present.

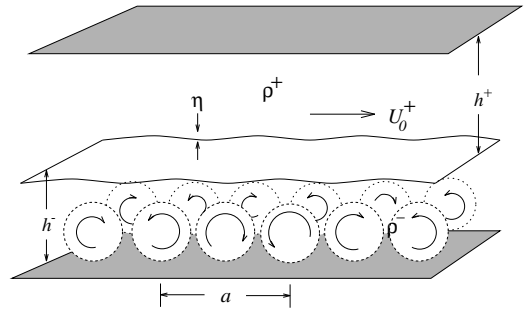


FIG. 1. Schematic of problem geometry. Two ideal fluids are separated by an interface with surface tension σ under the action of gravity. The densities, velocities, and depths of the upper and lower fluids are ρ^\pm , \vec{U}^\pm , and h^\pm respectively.

Formulation - Consider two ideal fluids separated by a flat wave-undisturbed interface at $z = 0$ as depicted in Fig. 1. Although the underlying flow field is typically rotational, we assume the flow associated with the imposed surface waves (externally excited) are irrotational. The displacements caused by the surface waves are assumed small and do not appreciably affect the underlying flow. This requirement, and linearization, implies $\eta \ll \lambda, a$ where η , λ , and a are typical surface amplitudes, wavelengths, and flow field periodicities respectively.

The fluid velocities above and below the interface are $\vec{v}^\pm = \vec{U}^\pm + \nabla\varphi^\pm$ where \vec{U} is the periodic flow field (generated for example, by the Rayleigh-Bénard instabilities [2], Langmuir circulation mechanisms [5], or electrohydrodynamic effects [10]) which satisfies $\nabla \cdot \vec{U} = 0$, and φ is the velocity potential for the irrotational capillary-gravity waves, and $z = \pm h^\pm$ is the position of the impenetrable top and bottom. For concreteness, consider the Rayleigh-Bénard system where instabilities to periodic flows in the Boussinesq approximation with a free surface arises when $\text{Ra} \equiv \alpha g h^3 \Delta T / (\nu \kappa) > \text{Ra}^*$, ($\text{Ra}^* \simeq 1100$ for a free, tensionless surface) where α , g , ΔT , ν , and κ are the thermal expansion coefficient, gravitational acceleration, temperature difference $T(z=0) - T(z=-h)$, kinematic viscosity, and thermal conductivity, respectively. The ideal fluid approximation is valid only for surface waves which are not significantly damped over many periods of the underlying flow, *i.e.*, for capillary waves, the attenuation length $k_d^{-1} \equiv 3\sigma / (4\nu\rho^{-\omega}) \gg a$. We also assume in this system a large Prandtl number such that the Reynolds number, $\text{Re} \sim \sqrt{\text{Ra}/\text{Pr}}$ is not too large as to render the steady periodic flows unstable.

Incompressibility demands $\nabla \cdot \vec{v} = \Delta\varphi = (\Delta_\perp + \partial_z^2)\varphi^\pm = 0$, where $\Delta \equiv \Delta_\perp + \partial_z^2$ is the three dimensional Laplacian. The boundaries at $z = \pm h^\pm$ are assumed flat and impenetrable. Therefore, the linearized kinematic boundary conditions at $z = \pm h^\pm$ and the interface at $z \simeq 0$ are $\partial_z\varphi^\pm(\vec{x}, z = \mp h) = 0$ and

$$\partial_t\eta(\vec{r}) + \vec{U}^\pm(\vec{r}) \cdot \nabla_\perp \eta(\vec{r}) = \lim_{z \rightarrow 0^\pm} \partial_z\varphi^\pm(\vec{r}, z) \quad (1)$$

respectively, where $\vec{r}_\perp \equiv \vec{r} \equiv (x, y)$. The linearized dynamical boundary condition at $z \simeq 0$ is found by balancing z -component stresses from the dynamical pressure with that from gravity and surface tension;

$$\lim_{z \rightarrow 0^\pm} [\partial_t\varphi^\pm + U^\pm \partial_i\varphi^\pm] = \frac{\sigma}{\rho^\pm} \Delta_\perp \eta - g\eta, \quad (2)$$

where we have for simplicity assumed a constant surface tension and neglected any possible Marangoni effects that may arise when surfactants are convected along the surface by $\vec{U}(\vec{r}, z=0)$. Spatially varying surface properties such as tension or bending rigidity can be treated without difficulty [9,11]. Henceforth, we assume that all quantities vary as $e^{-i\omega t}$. Wave evolution due to a non-time

harmonic source can be found by superposing the solutions of many frequency components. Consider general solutions to φ^\pm and $\eta(\vec{x})$,

$$\varphi^\pm(\vec{r}, z) = \sum_{\vec{q}} \varphi_{\vec{q}}^\pm e^{i\vec{q} \cdot \vec{r}} \frac{\cosh q(h^\pm \mp z)}{\cosh qh^\pm}, \quad (3)$$

and

$$\eta(\vec{r}) = \sum_{\vec{q}} \eta_{\vec{q}} e^{i\vec{q} \cdot \vec{r}} \quad (4)$$

where $\vec{q} \equiv \vec{q}_\perp$ lies in the surface plane, and $q \equiv \lim_{\epsilon \rightarrow 0} \sqrt{q^2 + \epsilon^2}$. Equation (3) automatically satisfies $\nabla^2\varphi = 0$ as well as the impenetrable bottom boundary condition. Therefore by using Eqn. (3), the problem is reduced to that of simultaneously solving equations (1) and (2) with the unknowns $\varphi_{\vec{q}}^\pm$ and $\eta_{\vec{q}}$. A Fourier decomposition for the periodic flows is

$$\vec{U}(\vec{r}, z) = \sum_{\vec{G}} \vec{U}(\vec{G}, z) e^{i\vec{G} \cdot \vec{r}}, \quad (5)$$

where \vec{G} is the reciprocal lattice vectors appropriate for the underlying flow periodicity. With the form (5), the velocity potential φ will furthermore be restricted to forms satisfying Bloch's theorem [8]: $\varphi(\vec{r} + \vec{a}, z) = e^{i\vec{q} \cdot \vec{r}} f(\vec{r}, z)$ where $f(\vec{r})$ is a function periodic with respect to translations of \vec{a} .

We wish to find the complex dispersion relation between ω and wavevector \vec{q} . Substituting Eqns. (3) and (4) into (1) and (2), we obtain

$$\varphi_{\vec{q}}^\pm = \pm \frac{1}{q \tanh qh^\pm} \left[i\omega\eta_{\vec{q}} - i \sum_{\vec{G}} \vec{U}^\pm(\vec{G}) \cdot (\vec{q} - \vec{G}) \eta_{\vec{q}-\vec{G}} \right] \quad (6)$$

and

$$s \left[-i\omega\varphi_{\vec{q}}^+ + i \sum_{\vec{G}} \vec{U}^+(\vec{G}) \cdot (\vec{q} - \vec{G}) \varphi_{\vec{q}-\vec{G}}^+ \right] + \left[i\omega\varphi_{\vec{q}}^- - i \sum_{\vec{G}} \vec{U}^-(\vec{G}) \cdot (\vec{q} - \vec{G}) \varphi_{\vec{q}-\vec{G}}^- \right] = \left(\frac{\sigma}{\rho} q^2 + g \right) \eta_{\vec{q}} \quad (7)$$

respectively. Shifting the the wavevector into the first Brillouin zone, and substituting (6) into (7), we find a generalized eigenvalue problem

$$\sum_{\vec{G}'} (\mathbf{A}\omega^2 + \mathbf{B}\omega + \mathbf{C}) \eta_{\vec{q}'}(\vec{G}') = 0 \quad (8)$$

where the matrices in the limit of unbounded upper fluid ($h^+ = \infty$, $h \equiv h^-$) are given by

$$A(\vec{G}, \vec{G}') \equiv (s \tanh |\vec{q} - \vec{G}|h + 1) \delta_{\vec{G}, \vec{G}'}, \quad (9)$$

$$B(\vec{G}, \vec{G}') \equiv -2s \vec{U}_0^+ \cdot (\vec{q} - \vec{G}) \tanh |\vec{q} - \vec{G}|h \delta_{\vec{G}, \vec{G}'}$$

$$- \left(1 + \frac{|\vec{q} - \vec{G}| \tanh |\vec{q} - \vec{G}|h}{|\vec{q} - \vec{G}'| \tanh |\vec{q} - \vec{G}'|h} \right) \vec{U}^-(\vec{G} - \vec{G}') \cdot (\vec{q} - \vec{G}')$$

$$(10)$$

$$C(\vec{G}, \vec{G}') \equiv \left(s |\vec{U}_0^+ \cdot (\vec{q} - \vec{G})|^2 \tanh |\vec{q} - \vec{G}|h - \Omega_q^2(\vec{G}) \right) \delta_{\vec{G}, \vec{G}'},$$

$$+ \sum_{\vec{G}''} \frac{|\vec{q} - \vec{G}| \tanh |\vec{q} - \vec{G}|h}{|\vec{q} - \vec{G}''| \tanh |\vec{q} - \vec{G}''|h} \vec{U}^-(\vec{G} - \vec{G}'') \cdot (\vec{q} - \vec{G}'')$$

$$\times \vec{U}^-(\vec{G}'' - \vec{G}') \cdot (\vec{q} - \vec{G}')$$

$$(11)$$

where $s \equiv \rho^+ / \rho^-$, and

$$\Omega_q^2(\vec{G}) = \left(\frac{\sigma}{\rho^-} |\vec{q} - \vec{G}|^3 + (1 - s)g |\vec{q} - \vec{G}| \right) \tanh |\vec{q} - \vec{G}|h$$

$$(12)$$

We arrive at an eigenvalue problem that can be solved by standard means [12],

$$\begin{pmatrix} \mathbf{0} & \mathbf{1} \\ -\mathbf{A}^{-1}\mathbf{C} & -\mathbf{A}^{-1}\mathbf{B} \end{pmatrix} \begin{pmatrix} \vec{\eta}_{\vec{q}} \\ \vec{\psi}_{\vec{q}} \end{pmatrix} = \omega \begin{pmatrix} \vec{\eta}_{\vec{q}} \\ \vec{\psi}_{\vec{q}} \end{pmatrix}, \quad (13)$$

where $\vec{\psi} \equiv \omega \vec{\eta}$. However, the above matrix is generally nonhermitian and the corresponding spectrum ω is complex. The standard criteria for the Kelvin-Helmholtz propagating wave instability is recovered when $\vec{U}^\pm = \vec{U}_0^\pm$ are uniform [13]:

$$(\omega - \vec{U}_0^- \cdot \vec{k})^2 + s \tanh kh (\omega - \vec{U}_0^+ \cdot \vec{k})^2 - \Omega_k^2(0) = 0. \quad (14)$$

Note that when dynamical effects of the upper fluid are neglected, ($s = 0$), the roots of Eqn. (14) are real, and no linear instability exists.

Results and Discussion - Distances, frequencies ω , and velocities U will be normalized and measured in units of a , $\sqrt{g/a}$, and \sqrt{ga} respectively. First consider only periodic flow in the lower fluid with no uniform component, $\vec{U}^\pm(\vec{G} = 0) = 0$. Only the velocity at the surface $\vec{U}^-(\vec{r}, z = 0)$ will influence surface wave propagation. For simplicity we only analyze one-dimensional rolls described by the approximate function,

$$\vec{U}^-(\vec{r}, z = 0) = U^-(z) \hat{x} \cos \left(\frac{2\pi}{a} x \right); \quad (15)$$

consequently, $\vec{U}^-(\vec{G}) = U^-(0) \hat{x} / 2\pi$ for $\vec{G} = \pm 2\pi \hat{x} / a$, and zero otherwise. This choice of phase for $\vec{U}^-(\vec{r}, z = 0)$

implies one converging and one diverging surface flow region per unit cell and also simplifies the computation by making all elements of the matrix in Eq. (13) real. Also, we choose small surface tensions so that the periodic flow surface velocities will be nonnegligible compared to water wave group velocities.

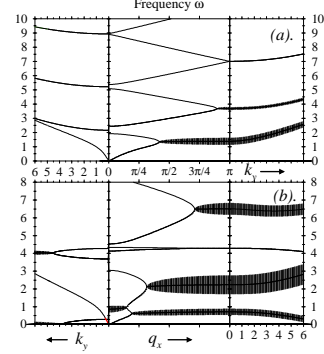


FIG. 2. Triptych depicting the band structure for periodic flow in the lower fluid ($s = 0$, $h = 2.0$, $\text{Bo}^{-1} = 0.01$). The central panel shows the dispersion relation in the q_x direction in the reduced zone scheme. (a). $U^-(2\pi/a) = 0.20$; (b). $U^-(2\pi/a) = 0.75$.

We find the spectrum of (13) using standard methods [12] and thus obtain the band structure of capillary-gravity waves on surfaces with underlying periodic flows \vec{U}^- . The central panels in Figures 2 show the real (solid lines) and imaginary (height of hatched regions centered about $\text{Re}\{\omega\}$) parts of $\omega(q_x, 0)$. We use the notation $q(k)$ to denote quantities plotted in the reduced(extended) zone scheme. The side panels show $\omega(0, k_y)$ for $\vec{U}_0^\pm = 0$, $h = 2.0$, $s = 0$, and the inverse Bond number $\text{Bo}^{-1} \equiv \sigma / (\rho^- a^2 g) = 0.01$. $U^-(\pm 2\pi/a) = 0.2, 0.75$ are shown in (a). and (b). respectively. The “band structures” shown in 2(a). contain branch cuts at certain q_x satisfying the Bragg scattering condition. There are open band gaps at $q_x = 0$, which decrease at larger ω , similar to electronic and acoustic wave propagation in periodic media; the gaps normally found at $q_x = \pm\pi$ are collapsed due to the converging flow in each unit cell and are degenerate down to a smaller value of q_x . Under this periodic flow, growing surface modes arise near $q_x \sim \pm\pi$ when real degenerate roots of Eqn. (13) split into complex conjugate pairs, even though for the one fluid problem,

uniform stream flows are stable according to (14). In Fig 2(b), $|U^-(\pm 2\pi/a)| = 0.75$ where the first gap at $q_x = 0$ has also merged. Note that unstable modes are associated with both standing and low group velocity travelling waves since they appear predominantly near $q_x = 0, \pi$. These may be damped or saturated by viscous dissipation, $\text{Im}\{\omega\} \simeq 2\nu|\vec{q} - \vec{G}|^2$. For $\vec{U}^-(2\pi/a) < 0.3641$, or higher values of surface tension, the band structure qualitatively resembles that of Fig. 2(a). At intermediate values of $\vec{U}^-(2\pi/a)$ (not shown), we find unstable nonoscillatory modes; *i.e.* $\text{Re}\{\omega(q_x, k_y)\} = 0, \text{Im}\{\omega(q_x, k_y)\} < 0$. When $0.417 > \vec{U}^-(2\pi/a) > 0.3641$, the lowest two branches collapse such that unstable zero frequency modes proliferate and fill the whole zone. These growing modes will be temporally saturated by viscosity and/or nonlinear effects, and result in static surface deformations similar to the Reynolds ridge [14]. Upon further increasing $\vec{U}^-(2\pi/a) > 0.417$, the zero frequency growing modes develop a finite frequency and stabilize near $q_x \sim 0$. When $\vec{U}^-(2\pi/a) \simeq 0.428$, the first gap at $q_x = 0$ between the stable modes collapse. The qualitative behavior described above continually repeats upon increasing $\vec{U}^-(2\pi/a)$. Note that for higher $U^-(2\pi/a)$ there are specific directions where oscillatory and nonoscillatory ($\text{Re}\{\omega(q_x, k_y)\} \rightarrow 0$) instabilities also arise.

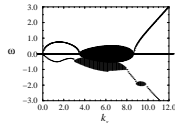


FIG. 3. Dispersion relation with and without an underlying periodic flow with a uniform ($\vec{U}_0^+ = 2.0$) overlying shear. Here, $h = \infty$, $\text{Bo}^{-1} = 0.03$, and $s = 0.1$. As a visual aid, we have imposed a k_x dependent Galilean shift $\Delta\vec{U}_0 = (\vec{U}_0^- + \vec{U}_0^+ s \tanh k_x h)/(1 + s \tanh k_x h)$. The pure shear dispersion ($\vec{U}^- = 0$) is shown by the dotted lines, with the imaginary parts of the unstable growing modes depicted by the heights of the hatched regions. The solid line ($\omega < 0$) defines the dispersion relation when a periodic flow ($\vec{U}^-(\vec{G} \neq 0) = 0.2$) is imposed. Note the changes to the instability regimes.

The band structures shown in Figures 2 are only quantitatively altered (tilted) when a small uniform shear is imposed in addition to the periodic flow. However, for uniform shear ($s = 0.1, h = \infty, U_0^+ = 2.6, \text{Bo}^{-1} = 0.1$) flows with an existing K-H instability (with un-

stable wavevectors near $k_x \sim \pi$) as determined by Eq. (14), the effect of an additional periodic flow in the lower fluid enhances these instabilities. However, when the uniform shear instabilities span $k_x \sim 2\pi$ ($s = 0.1, h = \infty, U_0^+ = 2.0, \text{Bo}^{-1} = 0.03$) where there is an open gap, the K-H instability can be *suppressed* by a periodic flow $U^-(2\pi/a) = 0.20$, although more instabilities arise at higher k_x as well. These effects are shown using the extended zone scheme in Figure 3. The structure of the dispersion relation is rather sensitive to the amount of underlying periodic flow and can change drastically with variation in any of the parameters.

Qualitatively, the upward convex tongue of the K-H instability in the $k_x - U_0^+$ plane is modified when $U^-(\vec{G} \neq 0)$ is added. For instabilities straddling the open gap Bragg planes, this tongue is shifted, with parts shifted upwards (resulting in destabilization) and downwards (resulting in stabilization). The discontinuity in growth rate is clearly shown in Fig. 3 near $k_x \simeq 2\pi$. Moreover, other smaller tongues develop at higher q_x ($k_x \simeq 3\pi$ in Fig. 3) corresponding to the closed gap instabilities that would occur in exclusively periodic flows (Fig. 2). The growth rates within the instability regions change as well as the delimiting instability regions. Qualitatively, these effects on K-H instabilities result from suppression of the travelling unstable waves in K-H shear flow, due to coupling to the standing waves of periodic flow, arising in the last term in \mathbf{C} in Eq. (11).

We have shown that periodic flows couple different reciprocal wavevectors together and affect interfacial stability in a nontrivial manner. In particular, by solving the matrix equations, we find, remarkably, that an interface overlying periodic flows is generally linearly unstable, *even if* $\rho^+ = 0$. The linear instabilities described would be saturated by both viscous and nonlinear effects. Regions of instability corresponding to finite frequency modes with vanishing group velocities, dissipation due to viscosity will result in a standing oscillating mode.

The analogies between wave propagation in periodic media and surface wave propagation in periodic shear flow configurations can be extended to consider more complicated periodic flow structures such as rectangular and hexagonal patterns, where rich behavior should be expected. This may lead to insights with wide applicability, from Rayleigh-Bénard convection, Langmuir circulation, solar convection cells, and MHD surface Alfvén waves in the presence of periodic magnetic fields (in addition to flows) [6]. Furthermore, the influence of defects and disorder in the periodic surface flows [15] can be considered to study surface wave localization in the presence of random $\vec{U}(\vec{r}, 0)$ (and hence random \mathbf{B}, \mathbf{C}). For example, methods used to determine the complex spectrum density of states of random matrix operators [16] should yield interesting behavior regarding the sea surface wave spectra in the presence of random underlying turbulent

- [1] A. D. D. Craik, *Wave interactions and fluid flows*, (Cambridge University Press, Cambridge, 1985).
- [2] L. G. Leal, *Laminar Flow and Convective Transport Processes*, (Butterworth-Heinemann, Boston, 1992). P. G. Drazin and W. H. Reid, *Hydrodynamic stability*, Cambridge monographs on mechanics and applied mathematics, (Cambridge University Press, 1981).
- [3] D. D. Joseph and Y. Y. Renardy, *Fundamentals of Two-Fluid Dynamics. Part I: Mathematical Theory and Applications*, (Springer-Verlag, New York, 1993); Y. Renardy and D. D. Joseph, *Phys. Fluids*, **28**, 788, (1985).
- [4] S. Leibovich, "The form and dynamics of Langmuir circulations," *Ann. Rev. Fluid Mech.*, **15**, 391-427, (1983).
- [5] C. J. R. Garrett, *J. Mar. Res.*, **34**, 117-130, (1976).
- [6] J. A. Shercliff, "Anisotropic surface waves under a vertical magnetic force," *J. Fluid Mech.*, **38**(2), 353-364, (1969).
- [7] R. D. Benguria and M. C. Depassier, *Phys. Fluids*, **30**(6), 1678-1682, (1987).
- [8] N. W. Ashcroft, and N. D. Mermin, *Solid State Physics*, (W. B. Saunders, Philadelphia, 1976); J. D. Joannopoulos, R. D. Meade, and J. Winn, *Photonic Crystals: Molding the Flow of Light*, (Princeton University Press, NJ, 1995).
- [9] T. Chou, "Band Gaps in Surface-Scattered Water Waves," submitted to *J. Fluid. Mech.*, (1997).
- [10] A. Ajdari, "Generation of transverse fluid currents and forces by an electric field: Electro-osmosis on charge-modulated and undulated surfaces," *Phys. Rev. E*, **53**(5), 4996-5005, (1996).
- [11] T. Chou and D. R. Nelson, "Surface wave scattering from nonuniform interfaces," *J. Chem. Phys.*, **101**(10), 9022-9032, (1994).
- [12] Press, W. H., Teukolsky, S. A., Vetterling, W. T., and Flannery, B. P., 1992. *Numerical Recipes*, (Cambridge, England).
- [13] B. Whitham, *Linear and Nonlinear Waves*, (Academic Press, 1973).
- [14] J. C. Scott, "Flow beneath a stagnant film on water: the Reynolds ridge," *J. Fluid. Mech.*, **116**, 283-296, (1982).
- [15] J. M. Massaguer, *Phys. Fluids*, **6**(7), 2304-2316, (1994). E. D. Siggia and A. Zippelius, *Phys. Rev A*, **24**(2), 1036-1049, (1981).
- [16] J. T. Chalker and Z. J. Wang, "Diffusion in a Random Velocity Field: Spectral Properties of a Non-Hermitian Fokker-Planck Operator," cond-mat/9704198